HHS Public Access

Author manuscript

AJR Am J Roentgenol. Author manuscript; available in PMC 2018 March 01.

Published in final edited form as:

AJR Am J Roentgenol. 2018 March ; 210(3): 621–628. doi:10.2214/AJR.17.18457.

MRI Features and *IDH* Mutational Status in Grade II Diffuse Gliomas: Impact on Diagnosis and Prognosis

Javier E. Villanueva-Meyer, **Matthew D. Wood**, **Byungse Choi**, **Marc C. Mabray**, **Nicholas A. Butowski**, **Tarik Tihan**, and **Soonmee Cha**

Department of Radiology and Biomedical Imaging (J.E.V., B.S.C., M.C.M., S.C.), Department of Pathology (M.D.W., T.T.), and Department of Neurological Surgery (N.A.B.), University of California San Francisco, San Francisco, California.

Abstract

BACKGROUND—Grade II diffuse gliomas (DGs) with isocitrate dehydrogenase (*IDH*) mutations are associated with better prognosis than their *IDH*-wildtype counterparts. We sought to determine MRI characteristics associated with *IDH* mutational status and whether MRI, combined with *IDH* mutational status, can better predict clinical outcomes of grade II DGs.

METHODS—Preoperative MRIs were retrospectively studied for qualitative tumor characteristics including location, extent, cortical involvement, margin sharpness, cystic component, mineralization or hemorrhage, and contrast enhancement. Quantitative diffusion and perfusion metrics were also assessed. Logistic regression and receiver operating characteristic analyses were used to evaluate the relationship between MRI features and *IDH* mutational status. The association between *IDH* mutational status, 1p19q co-deletion, MRI features, extent of resection, and clinical outcomes was assessed by Kaplan-Meier and Cox proportional hazards models.

RESULTS—Of 100 grade II DGs, 78 were *IDH*-mutant and 22 were *IDH*-wildtype. *IDH*-wildtype tumors were associated with older age, multifocality, brainstem involvement, lack of cystic change, and lower ADC. Multivariable regression showed that age >45 years as well as ADC_{min}, ADC_{mean}, and ADC_{max} were independently associated with *IDH* mutational status. Of these, an ADC_{min} threshold of 0.9×10^{-3} mm^2/s provided greatest sensitivity and specificity (91% and 76%, respectively) in defining *IDH*-wildtype grade II DGs. Combining low ADC_{min} with *IDH*-wildtype status conferred worse outcomes than *IDH*-wildtype status alone.

Correspondence to: Soonmee Cha.

Javier E. Villanueva-Meyer, 505 Parnassus, M-391, San Francisco CA 94143, 415-353-1668 (p), 415-353-2790 (f), javier.villanueva-meyer@ucsf.edu
Matthew D. Wood, 505 Parnassus, 551C, San Francisco CA 94143, 415-514-9332 (p), 415-476-7963 (f), matthew.wood@ucsf.edu
Byungse Choi, 505 Parnassus, M-391, San Francisco CA 94143, 415-353-1668 (p), 415-353-2790 (f), byungse.choi@gmail.com
Marc C. Mabray, 505 Parnassus, M-391, San Francisco CA 94143, 415-353-1668 (p), 415-353-2790 (f), mamabray@salud.unm.edu
Nicholas A. Butowski, 400 Parnassus, Box 0372, San Francisco CA 94143, 415-353-2383 (p), 415-353-2167 (f), nicholas.butowski@ucsf.edu
Tarik Tihan, 505 Parnassus, 551C, San Francisco CA 94143, 415-514-9332 (p), 415-476-7963 (f), tarik.tihan@ucsf.edu
Soonmee Cha, 350 Parnassus, 370H, San Francisco CA 94143, 415-353-8913 (p), 415-353-2790 (f), soonmee.cha@ucsf.edu

Conflict of Interest: None

This study was compliant with Health Insurance Portability and Accountability Act guidelines and was approved by the Institutional Review Board. The requirement for informed consent was waived.

CONCLUSION—*IDH*-wildtype grade II DGs are associated with lower ADC and poor clinical outcomes. Combining *IDH* mutational status and ADC may allow for more accurate prediction of clinical outcomes in patients with grade II DGs.

Keywords

low-grade glioma; grade II diffuse glioma; isocitrate dehydrogenase; IDH; MR

INTRODUCTION

Grade II DGs are a heterogeneous group of infiltrating glial neoplasms that includes astrocytomas, oligodendrogliomas, and oligoastrocytomas. These tumors have variable biology, treatment response, and prognosis [1–3]. Traditionally, classification of grade II DGs relied entirely upon histologic assessment [4]. However, recent advances in glioma genetics have led to the identification of several key molecular alterations in DGs [5,6]. The incorporation of these molecular markers in the 2016 World Health Organization Classification of Tumors of the CNS represents a paradigm shift from the isolated histopathologic assessment that had formed the basis of brain tumor classifications for nearly the past century [7]. These new guidelines emphasize *IDH* mutation as a key genetic alteration in the genesis of DGs and its role as a diagnostic and prognostic marker in patients with DGs.

Mutations in *IDH* occur early in oncogenesis and are found in the majority of DGs as well as in some non-glial tumors [8–10]. In grade II DGs, *IDH* mutational status defines two entities with distinct biologic behavior and clinical outcomes where the wildtype variant behaves more like a higher grade glioma with aggressive biology and worse outcomes when compared to the mutant variant [11–13]. This evidence, supported by the new World Health Organization classification, has resulted in increasing use of genetic markers to suggest pathologic diagnosis and guide clinical management [14,15]. Thus, discovering non-invasive imaging markers of *IDH* mutational status is an active area of investigation with potential high clinical impact for the diagnosis and therapeutic targeting of patients with DG. To date, physiologic MRI techniques, including DWI and PWI, have been extensively studied in gliomas and shown to be associated with tumor grade and outcomes [16–18]. While several studies have evaluated MRI characteristics as they relate to *IDH* mutational status, only a few have directly assessed grade II DGs. Yamashita et al and Lee et al have shown lower ADC values in *IDH*-wildtype glioblastoma and grade III and IV gliomas, respectively, and studies from Tan et al and Hempel et al have shown similar findings across grade II-IV gliomas (of which 25 were grade II in both studies) [19–22].

The purpose of our study was to 1) identify MRI markers predictive of *IDH* mutational status in grade II DGs and 2) evaluate the complementary roles of MRI features and *IDH* mutational status to better predict outcomes in these patients.

MATERIALS AND METHODS

Patients

Patients with histopathologically diagnosed grade II DG who underwent initial surgery at our institution over a four-year period (2010–2014) were included. All tissue samples were tested for *IDH* mutation as well as for loss of heterozygosity in chromosomes 1p and 19q (co-deletion). Other patient inclusion criteria were: age ≥18 years, treatment-naïve status, and no prior diagnosis of brain tumor. Patients were divided into two groups based on the presence of *IDH* mutation. Approval for this retrospective, HIPAA-compliant, study was obtained from our institutional review board.

Clinical and Pathologic Data

Patient demographics, extent of resection, adjuvant treatment, disease course, and survival data were collected from our electronic medical records. Progression free survival (PFS) and overall survival (OS) were calculated from date of initial surgery and endpoints were defined as date of progression by imaging and last follow-up or death, respectively.

Histopathologic evaluation was independently performed by two neuropathologists (M.W. and T.T.). *IDH* mutational status was determined by immunohistochemical antibody testing for *IDH1*-R132H mutation and, in 11 of the wildtype cases, further genomic sequencing analysis was performed to identify non-canonical mutations at the R132 codon in *IDH1* and R172 codon in *IDH2*. 1p/19q co-deletion was assessed by fluorescence in situ hybridization. Detailed methods for these molecular analyses have been described elsewhere [23,24].

MRI Protocol

Preoperative MRI was performed on a 3.0 Tesla system (Discovery; GE Healthcare, Waukesha, WI) including the following sequences: 3-plane localizer (TR/TE, 8.5/1.6 ms), sagittal T1-weighted spin-echo (TR/TE, 600/17 ms), axial 3D T2-weighted FSE (TR/TE, 3000/102 ms), 3D FLAIR (TR/TE/TI, 10000/148/2200 ms), axial DWI (TR/TE, 10000/99 ms; section thickness/intersection gap, 3/0 mm; matrix size 256 × 256 × 24; FOV 24 cm; b-value, 1000 s/mm^2), axial SWI (TR/TE, 43, 23 ms), axial DSC perfusion imaging (TR/TE, 1000–1250/54 ms; flip angle, 35°), and contrast-enhanced 3D SPGR T1-weighted imaging (TR/TE, 34/8 ms; section thickness/intersection gap, 1.5/0 mm). Contrast-enhanced sequences were obtained after using a gadolinium-based contrast agent (Gadavist, gadobutrol; Bayer HealthCare, Berlin, Germany) dosed at 0.1 mL/kg.

Qualitative MRI Characteristics

Tumors were characterized by extent and primary site of involvement. Multifocal tumor was defined as involvement two or more sites connected by direct routes of spread such as along white matter tracts or subependymal spread. Multicentric tumor was defined as involvement of multiple sites not connected by obvious routes of spread. Primary site of involvement was characterized as lobar (cerebrum and cerebellum), central (insula, basal ganglia, thalamus, and hypothalamus), or brainstem.

Readers recorded the presence or absence of the following conventional MRI characteristics in a binary fashion: 1) cortical involvement, 2) indistinct margins, 3) mineralization or hemorrhage, 4) cystic change, and 5) contrast enhancement. Cortical involvement was defined as any expansile T2 signal abnormality or contrast enhancement in the cerebral cortex. Tumor margins were categorized as indistinct based on ill-defined and irregular perimeter on FLAIR. Mineralization or hemorrhage were identified as intratumoral foci of susceptibility on SWI. Cystic change was defined as circumscribed T2 hyperintense non-enhancing foci within the tumor.

Quantitative MRI Measurements

The FLAIR, DWI, DSC, and contrast-enhanced 3D SPGR images were transferred to a commercially available workstation (Advantage Workstation version 4.6; GE Healthcare) for processing of DWI and DSC using FuncTool (version 4.6; GE Healthcare). The FLAIR and contrast-enhanced 3D SPGR images were aligned to the same transaxial location and resolution as the DWI images and ADC maps were generated on a voxel-by-voxel basis from the diffusion imaging sets. For DSC calculations, T2* DSC images were utilized to produce CBV maps and corresponding T2* susceptibility signal intensity-time curves on a voxel-by-voxel basis after segmenting the area of interest. FLAIR and contrast-enhanced 3D SPGR images were then aligned with the T2* DSC images. ROIs were then manually delineated about the tumor at all available axial planes. Care was taken to avoid cysts, necrosis, mineralization, hemorrhage, or vasculature that could have effects on physiologic MRI measurements. ROIs were transferred to ADC and CBV maps allowing for collection of ADC_{min}, ADC_{mean}, and ADC_{max} as well as CBV_{mean} and CBV_{max}. The individual ROI values were weighted by ROI area to calculate the average of the mean ADC and CBV from the entirety of tumor. Perfusion were standardized to a 50 mm^2 ROI placed on the contralateral normal-appearing white matter to produce relative imaging values ($rCBV_{mean}$ and $rCBV_{max}$).

MRI features were assessed independently by two board-certified neuroradiologists (B.C. and S.C., 10 and 15 years of experience, respectively) blinded to clinical and pathologic information. In case of disagreement, consensus interpretation was performed. Quantitative assessment on the Advantage workstation was performed by a board-eligible neuroradiologist (J.E.V., 5 years of experience and additional training by the software provider).

Statistical Analysis

Differences in clinical and MRI features between *IDH*-mutant and *IDH*-wildtype groups were analyzed using the chi-square test for categorical variables and Mann-Whitney *U* test for continuous variables. Inter-rater reliability was assessed with Cohen's kappa and intra-class correlation coefficients for categorical and continuous data, respectively. Inter-rater reproducibility was interpreted as 0–0.2, slight; 0.21–0.4, fair; 0.41–0.6, moderate; 0.61–0.8, substantial; and 0.81–1, near-perfect according to previously described methods [25]. Receiver operating characteristic was applied and logistic regression modeling was performed and to determine the ability of variables to discriminate *IDH* mutational status. Cox proportional hazards models were computed using *IDH* and MRI characteristics to

assess the relationship between *IDH* mutational status, 1p19q co-deletion, MRI characteristics, extent of resection, and clinical outcomes. Kaplan-Meier survival curves were generated to estimate PFS and OS and log-rank tests were performed to evaluate differences between tumor groups. *P*-values of less than or equal to 0.05 were considered statistically significant. Statistical analyses were performed using commercially-available software (Medcalc version 16.1; Ostend, Belgium).

RESULTS

Patient Demographics

Of the 100 included patients, 78 had *IDH*-mutant and 22 had *IDH*-wildtype grade II DGs. Patients with *IDH*-wildtype tumors were older at time of diagnosis compared to patients with *IDH*-mutant tumors (median age 58 versus 41, $p = 0.004$). No significant differences were seen in gender between the two groups. No significant difference was observed in gross total resection between *IDH*-mutant (24; 31%) and *IDH*-wildtype (7; 32%) tumors ($p = 0.925$). Significantly more *IDH*-mutant (41; 52%) tumors underwent subtotal resection when compared to *IDH*-wildtype (5, 23%) tumors ($p = 0.025$). Significantly more *IDH*-wildtype (10; 45%) tumors underwent biopsy alone than *IDH*-mutant (13; 17%) tumors ($p = 0.011$).

MRI Characteristics

Representative MRIs of the two tumor groups are depicted in Figure 1. Table 1 summarizes qualitative MRI findings. *IDH*-wildtype tumors were more often multifocal ($p = 0.004$). All studied brainstem tumors were *IDH*-wildtype ($p < 0.001$). No significant difference in frequency of *IDH* mutation was seen in tumors with lobar or central location. Cystic change was seen less frequently in *IDH*-wildtype tumors ($p = 0.033$). There was a trend toward lower frequency of cortical involvement in *IDH*-wildtype tumors that did not meet statistical significance ($p = 0.069$). No significant correlation was noted between *IDH* mutation and the other studied morphologic variables including indistinct margins, mineralization or hemorrhage, or contrast enhancement. Quantitative MRI parameters are depicted graphically in Figure 2 and Figure 3. ADC_{min}, ADC_{mean}, ADC_{Mmax} measurements were significantly lower in *IDH*-wildtype compared to *IDH*-mutant grade II DGs ($p < 0.001$). No significant difference was noted in either $rCBV_{mean}$ or $rCBV_{max}$ between tumor groups.

There was suitable agreement between readers for morphologic MRI characteristics of cortical involvement, tumor margin, cystic change, mineralization or hemorrhage, and contrast enhancement (Cohen's kappa = 0.87, 0.77, 0.77, 0.93, 0.91, respectively). Inter-reader agreement was at least substantial for ADC and rCBV measurements (intra-class correlation coefficient range 0.71 – 0.91) and was highest for ADC_{min} (intra-class correlation coefficient = 0.91).

Regression

Patient age >45 years, multifocal tumor, brainstem location, absence of cystic change as well as low ADC_{min}, ADC_{mean}, and ADC_{max} (threshold values ≤ 0.9, 1.28, 1.75×10^{-3} mm^2/s, respectively) were found to be independent predictors of *IDH* wildtype status. Of these,

ADC_{min} was found to have the greatest AUC (0.905, 95% CI = 0.830 – 0.954, $p < 0.001$) with an ADC_{min} threshold of $\leq 0.9 \times 10^{-3}$ mm^2/s (low ADC_{min}) corresponding to a sensitivity of 90.9% and a specificity of 75.6% for *IDH*-wildtype status.

Multiple-variable logistic regression analyses for the identification of *IDH*-wildtype DGs using each ADC variable (ADC_{min}, ADC_{mean}, and ADC_{max}) threshold in combination with the other independent variables were statistically significant (overall models $p < 0.001$). Separate analyses were performed for each ADC variable due to multicollinearity. Individually, the ADC variables (ADC_{min} coefficient = 2.99, $p < 0.001$; ADC_{mean} coefficient = 1.51, $p = 0.029$; ADC_{max} coefficient = 1.72, $p = 0.043$) and age >45 years (coefficient = 1.96, $p = 0.008$; coefficient = 1.84, $p = 0.008$; coefficient = 1.92, $p = 0.005$, for each ADC variable respectively) remained significant. The other independent variables were not significant.

Clinical outcomes

The mean follow-up period was 38.6 ± 19.7 months. By the time of the last assessment, 47 of 100 had tumor progression (17 of 22 *IDH*-wildtype and 30 of 78 *IDH*-mutant) and 18 of 100 had died (12 of 22 *IDH*-wildtype and 6 of 78 *IDH*-mutant, all secondary to glioma). The median PFS of all patients was 42.0 months. As survival probability did not drop below 0.5, median OS was not computed. The mean OS of all patients was 74.0 months.

The median PFS of the *IDH*-wildtype group (27.0 months; 95% CI, 12.6 – 41.5 months) was significantly shorter than that of the *IDH*-mutant group (46.0 months; 95% CI, 37.7 – 70.7 months). *IDH*-wildtype status conferred a hazard ratio of 2.50 (95% CI, 1.37 – 4.57; $p = 0.005$) for progression. The mean OS of the *IDH*-wildtype group (45.9 months; 95% CI, 34.0 – 57.8 months) was also significantly shorter than that of the *IDH*-mutant group (78.3 months; 95% CI, 65.1 – 91.5 months). *IDH*-wildtype status conferred a hazard ratio of 6.14 (95% CI, 2.25 – 16.74; $p < 0.001$) for death. Kaplan-Meier curves of PFS and OS between the groups are shown in Figure 4.

The median PFS when stratified by 1p19q co-deletion was significantly shorter for tumors without 1p19q co-deletion (30.8 months; 95% CI, 25.4 – 42.0) compared to tumors with 1p19q co-deletion (70.7 months; 95% CI, 42.6 – 60.9) ($p = 0.009$). Absence of 1p19q co-deletion conferred a hazard ratio of 2.29 (95% CI, 1.12 – 4.30; $p = 0.011$) for progression. The mean OS when stratified by 1p19q co-deletion was significantly shorter for tumors without 1p19q co-deletion (63.7 months; 95% CI, 53.90 – 73.58) compared to tumors with 1p19q co-deletion (85.90 months; 95% CI, 73.50 – 98.29) ($p = 0.007$). Absence of 1p19q co-deletion conferred a hazard ratio of 5.95 (95% CI, 1.36 – 26.0; $p = 0.018$) for death.

The median PFS of the tumors that underwent gross total resection (50.5 months; 95% CI, 44.2 – 56.8 months) was significantly longer than that underwent subtotal resection (42.6 months; 95% CI, 30.8 – 57.6 months) or biopsy alone (21.6 months; 95% CI, 13.5 – 34.7) ($p < 0.001$). Subtotal resection conferred a hazard ratio of 2.27 (95% CI, 1.19 – 4.33; $p < 0.001$) and biopsy conferred a hazard ratio of 4.87 (95% CI, 2.20 – 10.75; $p < 0.001$) for progression. The mean OS of the tumors that underwent gross total resection (85.4 months; 95% CI, 80.3 – 90.6 months) was significantly longer than that underwent subtotal resection

(65.3 months; 95% CI, 59.5 – 71.2 months) or biopsy alone (54.3 months; 95% CI, 39.9 – 68.6) ($p < 0.001$). Subtotal resection conferred a hazard ratio of 3.44 (95% CI, 1.12 – 10.55; $p < 0.001$) and biopsy conferred a hazard ratio of 13.0 (95% CI, 3.63 – 46.57; $p < 0.001$) for death.

The independent contributions of age and ADC_{min} $ADC_{min} \leq 0.9 \times 10^{-3}$ mm^2/s conferred a hazard ratio of 1.84 (95% CI, 1.03 – 3.29; $p = 0.039$) for progression and a hazard ratio of 2.88 (95% CI, 1.00 – 8.24; $p = 0.040$) for death. Cox proportional hazards regression did not show age > 45 years to be significant for PFS ($p = 0.555$) or OS ($p = 0.227$).

MRI features with clinical outcomes

Using the studied variables, Cox proportional-hazards regression modeling with patients stratified by *IDH* mutational status and ADC_{min} (threshold $\leq 0.9 \times 10^{-3}$ mm^2/s to define low versus high ADC_{min}) demonstrated greater risk of negative outcomes in patients with *IDH* mutational status and low ADC_{min}. For PFS (overall fit, $p = 0.016$), *IDH*-wildtype and low ADC_{min} conferred a hazard ratio of 2.77 (95% CI, 1.36 – 5.61; $p = 0.005$) for tumor progression. For OS (overall fit, $p = 0.002$), *IDH*-wildtype and low ADC_{min} conferred a hazard ratio of 6.41 (95% CI, 1.77 – 23.26; $p = 0.005$) for death. Other comparisons between *IDH* mutational status and ADC_{min} were not significant.

DISCUSSION

Our study identified older age, multifocality, brainstem involvement, lack of cystic change, and low ADC as independent predictors of *IDH*-wildtype grade II DGs. Among these, ADC_{min} was most predictive with a threshold of $\leq 0.9 \times 10^{-3}$ mm^2/s conferring the greatest sensitivity (91%). Furthermore, while shorter PFS and OS were seen in *IDH*-wildtype grade II DGs, combining *IDH* status and ADC_{min} better predicted PFS and OS than *IDH* status alone.

Advances in our understanding of gliomagenesis highlight the importance of *IDH* mutations in predicting the clinical behavior of DGs [5,6,26–29]. The most recent revision of the 4th World Health Organization Classification of Tumors of the CNS introduces the concept of “integrated diagnosis,” which incorporates key genetic and molecular alterations, including *IDH* mutations, in the final pathologic diagnosis [7]. Special testing has become almost mandatory to formulate this integrated diagnosis, which may pose a significant challenge when these analytical tests are not readily available. Therefore, MRI can provide an advantage in the detection of these genetic characteristics indirectly and, as these tests become standard-of-care, radiology has the potential to serve an adjunctive role alongside the integrated pathologic diagnosis.

Here, we found lower ADC_{min}, ADC_{mean}, and ADC_{max} were predictive of *IDH* mutation in grade II DGs with an ADC_{min} threshold of $\leq 0.9 \times 10^{-3}$ mm^2/s, as most sensitive for defining *IDH*-wildtype status. Given the aggressive biology demonstrated by *IDH*-wildtype tumors, and taking into consideration literature demonstrating an inverse relationship between ADC and outcomes, our findings suggest that ADC_{min} can be used to predict prognosis of grade II DGs. The observed differences in ADC of glioma have been ascribed

to increased cellularity and/or neovascularization associated with higher grade tumors. Cell culture experiments have shown that *IDH*-mutant cells demonstrate reduced proliferation and form looser aggregates in culture when compared to *IDH*-wildtype cells [30,31]. Given these in vitro findings, we hypothesize that regions of low diffusivity seen in *IDH*-wildtype DGs represent sites of elevated cellular density or increased grade. Due to the heterogeneity often observed within the same tumor, we believe that ADC_{min} presents a more robust measure of tumor aggressiveness as whole-tumor statistics (e.g. ADC_{mean}) may mask the true characteristics of the tumor. Furthermore, our findings of shorter PFS and OS in *IDH*-wildtype grade II DGs recapitulate the findings seen in studies of grade II-IV gliomas [5,6,32]. While we additionally found that low ADC_{min} was independently associated with worse outcomes, combining low ADC_{min} with *IDH* status better predicted both PFS and OS of DG patients. Notably, patients with *IDH*-wildtype DGs who had low ADC_{min} ($\leq 0.9 \times 10^{-3}$ mm^2/s) had shorter PFS and and OS than *IDH*-mutant DG patients. This suggests that the combination of low ADC_{min} and *IDH*-wildtype status may reflect a higher malignant potential of DGs harboring these characteristics and is consistent with their status as independent surrogates of outcome.

In contradistinction to DWI, we observed a large degree of overlap in rCBV between *IDH*-mutant and *IDH*-wildtype grade II gliomas. While a number of studies have shown differences in PWI across glioma grades, several have also shown differences between histologic subtypes, notably, oligodendroglial tumors have been shown to have elevated rCBV compared to diffuse astrocytomas [33–35]. Our observed lack of difference in rCBV based on *IDH* mutational status may reflect several underlying factors including tumor heterogeneity, site of tumor, as well as variation in histologic subtypes between the groups. Additionally, some investigators have shown the predictive value of PWI, among other MR techniques, to detect transformation of a low to high grade glioma [17,34]. Longitudinal evaluation with perfusion metrics was beyond the scope of this study, however, such evaluation would be of clinical interest.

We observed variability in structural MRI findings with significant differences in tumor location and cystic change between the *IDH*-mutant and *IDH*-wildtype DGs. Specifically, all of the brainstem tumors in our study were *IDH*-wildtype. This finding may be to be related to the greater prevalence of purely astrocytic tumors in the *IDH*-wildtype group and the possibility of undiagnosed histone H3 K27M mutated gliomas, for which testing was not routinely performed at our institution during the study period [36]. Our findings support those of Qi et al who showed greater incidence of central and infratentorial location of *IDH*-wildtype gliomas [37]. The increased incidence of cystic change in the *IDH*-mutant cohort may reflect the higher proportion of tumors with oligodendroglial histology seen in this study as cystic change is frequently noted in oligodendrogliomas [38].

Oligodendrogliomas are now defined by the WHO as a diffusely infiltrating glioma with *IDH* mutation and co-deletion of 1p19q. Co-deletion of 1p19q trumps histologic features to definitively diagnose and distinguish oligodendrogliomas from other glial neoplasms and portends a favorable response to therapy and prognosis [5,39]. In our studied patients, none of *IDH*-wildtype tumors were 1p19q co-deleted, suggesting that *IDH*-wildtype tumors are, regardless of their histologic features, not molecular and genetic oligodendrogliomas but

more likely to represent higher grade astrocytomas. are in line with prior studies and emphasize the relevance of molecular markers in diagnosing and prognosticating DGs.

Extent of resection is a well-known important determinant of prognosis [40,41]. At our institution, the standard of care neurosurgical approach to DGs is maximal safe resection as permitted by size and location of the tumor. As expected and supported by published reports, we found improved PFS and OS in patients who had gross total resection of tumor when compared to subtotal resection or biopsy. While there were differences in tumor location between *IDH*-wildtype and *IDH*-mutant tumors, which can be assumed to account for the increased frequency of biopsy alone in the *IDH*-wildtype tumors, no difference was observed between the two groups when comparing by gross total resection. That we found significantly improved outcomes following gross total resection in this context highlights the added importance of *IDH* mutational as an independent prognostic marker in DGs.

Lastly, we found that patients harboring *IDH*-wildtype tumors were 10 years older on average than those with *IDH* mutant tumors and that age > 45 years was predictive of *IDH*-wildtype tumor. These findings are consistent with recently published literature in large patient cohorts [5,6]. Although we did not see a significant difference in outcomes when stratified by age > 45, age is a known prognostic factor in gliomas and the relationship between patient age, among other clinical factors, *IDH* status, and outcomes should be considered further.

The main strengths of our study are its sample size, the isolation of grade II DGs, and correlation between *IDH*-mutational status, MRI findings, and outcomes. However, its retrospective design and single center sampling remain limitations, particularly to power more robust multivariate analysis. Further prospective studies with multicenter patient populations are warranted for validation of our findings and to incorporate additional variables for analysis. Additionally, undersampling may have led to incomplete tumor characterization including undergrading. Furthermore, other genetic alterations including ATRX and TERT mutations as well as EGFR expression and *PTEN* mutations were not consistently assessed and a proportion of the midline tumors may have represented histone H3 K27M mutant DGs. It should also be noted that detection of accumulated 2-hydroxyglutarate seen in *IDH*-mutant tumors by MR spectroscopy is a promising new tool in the non-invasive characterization of glioma, however, as this requires optimized techniques not typically available on clinical scanners and was not routinely performed in our cohort, we did not assess this in our study [42–44]. As molecular testing becomes routine and our imaging techniques improve, future studies could address these limitations and image-guided tissue sampling could directly correlate imaging characteristics with histology and molecular markers.

In conclusion, *IDH*-wildtype grade II DGs represent a clinically aggressive type of DGs that can be recognized by quantitative DWI. Specifically, ADC_{min} with a threshold of $\leq 0.9 \times 10^{-3}$ mm^2/s is an imaging predictor of *IDH*-wildtype DGs and combining *IDH* mutational status with ADC metrics may provide a more accurate predictor of survival. MRI biomarkers can be further validated in studies that analyze *IDH* mutations, and may improve clinical risk

stratification, guide personalized therapeutic strategy and assess clinical outcomes in patients with DG.

Acknowledgments

Funding: J.E.V. was supported by a US Department of Health and Human Services - National Institutes of Health - National Institute of Biomedical Imaging and Bioengineering (5T32EB001631-12)

References

1. Yeh SA, Ho JT, Lui CC, et al. Treatment outcomes and prognostic factors in patients with supratentorial low-grade gliomas. Br J Radiol. 2005; 78:230–235. [PubMed: 15730987]
2. Sanai N, Chang S, Berger MS. Low-grade gliomas in adults. J Neurosurg. 2011; 115:948–965. [PubMed: 22043865]
3. Claus EB, Walsh KM, Wiencke JK, et al. Survival and low-grade glioma: the emergence of genetic information. Neurosurg Focus. 2015; 38:E6.
4. Louis DN, Ohgaki H, Wiestler OD, et al. The 2007 WHO Classification of Tumours of the Central Nervous System. Acta Neuropathol. 2007; 114:97–109. [PubMed: 17618441]
5. Eckel-Passow JE, Lachance DH, Molinaro AM, et al. Glioma Groups Based on 1p/19q, IDH, and TERT Promoter Mutations in Tumors. N Engl J Med. 2015; 372:2499–2508. [PubMed: 26061753]
6. Brat DJ, Verhaak RGW, et al. Cancer Genome Atlas Research Network. Comprehensive, Integrative Genomic Analysis of Diffuse Lower-Grade Gliomas. N Engl J Med. 2015; 372:2481–2498. [PubMed: 26061751]
7. Louis DN, Perry A, Reifenberger G, et al. The 2016 World Health Organization Classification of Tumors of the Central Nervous System: a summary. Acta Neuropathol. 2016; 131:803–820. [PubMed: 27157931]
8. Ichimura K. Molecular pathogenesis of IDH mutations in gliomas. Brain Tumor Pathol. 2012; 29:131–139. [PubMed: 22399191]
9. Juratli TA, Kirsch M, Robel K, et al. IDH mutations as an early and consistent marker in low-grade astrocytomas WHO grade II and their consecutive secondary high-grade gliomas. J Neurooncol. 2012; 108:403–410. [PubMed: 22410704]
10. Yan H, Parsons DW, Jin G, et al. IDH1 and IDH2 mutations in gliomas. N Engl J Med. 2009; 360:765–773. [PubMed: 19228619]
11. Houillier C, Wang X, Kaloshi G, et al. IDH1 or IDH2 mutations predict longer survival and response to temozolomide in low-grade gliomas. Neurology. 2010; 75:1560–1566. [PubMed: 20975057]
12. Metellus P, Coulibaly B, Colin C, et al. Absence of IDH mutation identifies a novel radiologic and molecular subtype of WHO grade II gliomas with dismal prognosis. Acta Neuropathol. 2010; 120:719–729. [PubMed: 21080178]
13. Leu S, Felten von S, Frank S, et al. IDH/MGMT-driven molecular classification of low-grade glioma is a strong predictor for long-term survival. Neuro Oncol. 2013; 15:469–479. [PubMed: 23408861]
14. Le Rhun E, Taillibert S, Chamberlain MC. Current Management of Adult Diffuse Infiltrative Low Grade Gliomas. Curr Neurol Neurosci Rep. 2016; 16:15. [PubMed: 26750130]
15. Duffau H, Taillandier L. New concepts in the management of diffuse low-grade glioma: Proposal of a multistage and individualized therapeutic approach. Neuro Oncol. 2015; 17:332–342. [PubMed: 25087230]
16. Tozer DJ, Jäger HR, Danchaivijitr N, et al. Apparent diffusion coefficient histograms may predict low-grade glioma subtype. NMR Biomed. 2007; 20:49–57. [PubMed: 16986106]
17. Law M, Young RJ, Babb JS, et al. Gliomas: Predicting Time to Progression or Survival with Cerebral Blood Volume Measurements at Dynamic Susceptibility-weighted Contrast-enhanced Perfusion MR Imaging 1. Radiology. 2008; 247:490–498. [PubMed: 18349315]

18. Zulfiqar M, Yousem DM, Lai H. ADC values and prognosis of malignant astrocytomas: does lower ADC predict a worse prognosis independent of grade of tumor?--a meta-analysis. AJR Am J Roentgenol. 2013; 200:624–629. [PubMed: 23436853]
19. Yamashita K, Hiwatashi A, Togao O, et al. MR Imaging-Based Analysis of Glioblastoma Multiforme: Estimation of IDH1 Mutation Status. AJNR Am J Neuroradiol. 2016; 37:58–65. [PubMed: 26405082]
20. Lee S, Choi SH, Ryoo I, et al. Evaluation of the microenvironmental heterogeneity in high-grade gliomas with IDH1/2 gene mutation using histogram analysis of diffusion-weighted imaging and dynamic-susceptibility contrast perfusion imaging. J Neurooncol. 2015; 121:141–150. [PubMed: 25205290]
21. Tan WL, Huang WY, Yin B, et al. Can Diffusion Tensor Imaging Noninvasively Detect IDH1 Gene Mutations in Astrogliomas? A Retrospective Study of 112 Cases. AJNR Am J Neuroradiol. 2014; 35:920–927. [PubMed: 24557705]
22. Hempel JM, Bisdas S, Schittenhelm J, et al. In vivo molecular profiling of human glioma using diffusion kurtosis imaging. J Neurooncol. 2017; 131:93–101. [PubMed: 27604789]
23. van den Bent MJ, Hartmann C, Preusser M, et al. Interlaboratory comparison of IDH mutation detection. J Neurooncol. 2013; 112:173–178. [PubMed: 23358936]
24. Horbinski C, Miller CR, Perry A. Gone FISHing: clinical lessons learned in brain tumor molecular diagnostics over the last decade. Brain Pathol. 2011; 21:57–73. [PubMed: 21129060]
25. Landis JR, Koch GG. The measurement of observer agreement for categorical data. Biometrics. 1977; 33:159–174. [PubMed: 843571]
26. Hartmann C, Hentschel B, Wick W, et al. Patients with IDH1 wild type anaplastic astrocytomas exhibit worse prognosis than IDH1-mutated glioblastomas, and IDH1 mutation status accounts for the unfavorable prognostic effect of higher age: implications for classification of gliomas. Acta Neuropathol. 2010; 120:707–718. [PubMed: 21088844]
27. Kim Y-H, Nobusawa S, Mittelbronn M, et al. Molecular Classification of Low-Grade Diffuse Gliomas. Am J Pathol. 2010; 177:2708–2714. [PubMed: 21075857]
28. Hartmann C, Hentschel B, Tatagiba M, et al. Molecular Markers in Low-Grade Gliomas: Predictive or Prognostic? Clin Cancer Res. 2011; 17:4588–4599. [PubMed: 21558404]
29. Jiao Y, Killela PJ, Reitman ZJ, et al. Frequent ATRX, CIC, FUBP1 and IDH1 mutations refine the classification of malignant gliomas. Oncotarget. 2012; 3:709–722. [PubMed: 22869205]
30. Kessler J, Güttler A, Wichmann H, et al. IDH1R132H mutation causes a less aggressive phenotype and radiosensitizes human malignant glioma cells independent of the oxygenation status. Radiother Oncol. 2015; 116:381–387. [PubMed: 26328938]
31. Cui D, Ren J, Shi J, et al. R132H mutation in IDH1 gene reduces proliferation, cell survival and invasion of human glioma by downregulating Wnt/β-catenin signaling. Int J Biochem Cell Biol. 2016; 73:72–81. [PubMed: 26860959]
32. Wang K, Wang Y, Fan X, et al. Radiological features combined with IDH1status for predicting the survival outcome of glioblastoma patients. Neuro Oncol. 2016; 18:589–597. [PubMed: 26409566]
33. Cha S, Tihan T, Crawford F, et al. Differentiation of low-grade oligodendrogliomas from low-grade astrocytomas by using quantitative blood-volume measurements derived from dynamic susceptibility contrast-enhanced MR imaging. AJNR Am J Neuroradiol. 2005; 26:266–273. [PubMed: 15709123]
34. Essig M, Nguyen TB, Shiroishi MS, et al. Perfusion MRI: The Five Most Frequently Asked Clinical Questions. AJR Am J Roentgenol. 2013; 201:W495–W510. [PubMed: 23971482]
35. Griffith B, Jain R. Perfusion Imaging in Neuro-Oncology. Radiol Clin North Am. 2015; 53:497–511. [PubMed: 25953286]
36. Solomon DA, Wood MD, Tihan T, et al. Diffuse Midline Gliomas with Histone H3-K27M Mutation: A Series of 47 Cases Assessing the Spectrum of Morphologic Variation and Associated Genetic Alterations. Brain Pathol. 2016; 26:569–580. [PubMed: 26517431]
37. Qi S, Yu L, Li H, et al. Isocitrate dehydrogenase mutation is associated with tumor location and magnetic resonance imaging characteristics in astrocytic neoplasms. Oncol Lett. 2014; 7:1895–1902. [PubMed: 24932255]

38. Koeller KK, Rushing EJ. From the archives of the AFIP: Oligodendroglioma and its variants: radiologic-pathologic correlation. Radiographics. 2005; 25:1669–1688. [PubMed: 16284142]

39. Leeper HE, Caron AA, Decker PA, et al. IDH mutation, 1p19q codeletion and ATRX loss in WHO grade II gliomas. Oncotarget. 2015; 6:30295–30305. [PubMed: 26210286]

40. Almeida JP, Chaichana KL, Rincon-Torroella J, et al. The Value of Extent of Resection of Glioblastomas: Clinical Evidence and Current Approach. Curr Neurol Neurosci Rep. 2014; 15:517.

41. Hervey-Jumper SL, Berger MS. Maximizing safe resection of low- and high-grade glioma. J Neurooncol. 2016; 130:269–282. [PubMed: 27174197]

42. Andronesi OC, Kim GS, Gerstner E, et al. Detection of 2-hydroxyglutarate in IDH-mutated glioma patients by in vivo spectral-editing and 2D correlation magnetic resonance spectroscopy. Sci Transl Med. 2012; 4:116ra4.

43. Choi C, Ganji SK, DeBerardinis RJ, et al. 2-hydroxyglutarate detection by magnetic resonance spectroscopy in IDH-mutated patients with gliomas. Nat Med. 2012; 18:624–629. [PubMed: 22281806]

44. Nagashima H, Tanaka K, Sasayama T, et al. Diagnostic value of glutamate with 2-hydroxyglutarate in magnetic resonance spectroscopy forIDH1mutant glioma. Neuro Oncol. 2016; 18:1559–1568. [PubMed: 27154922]

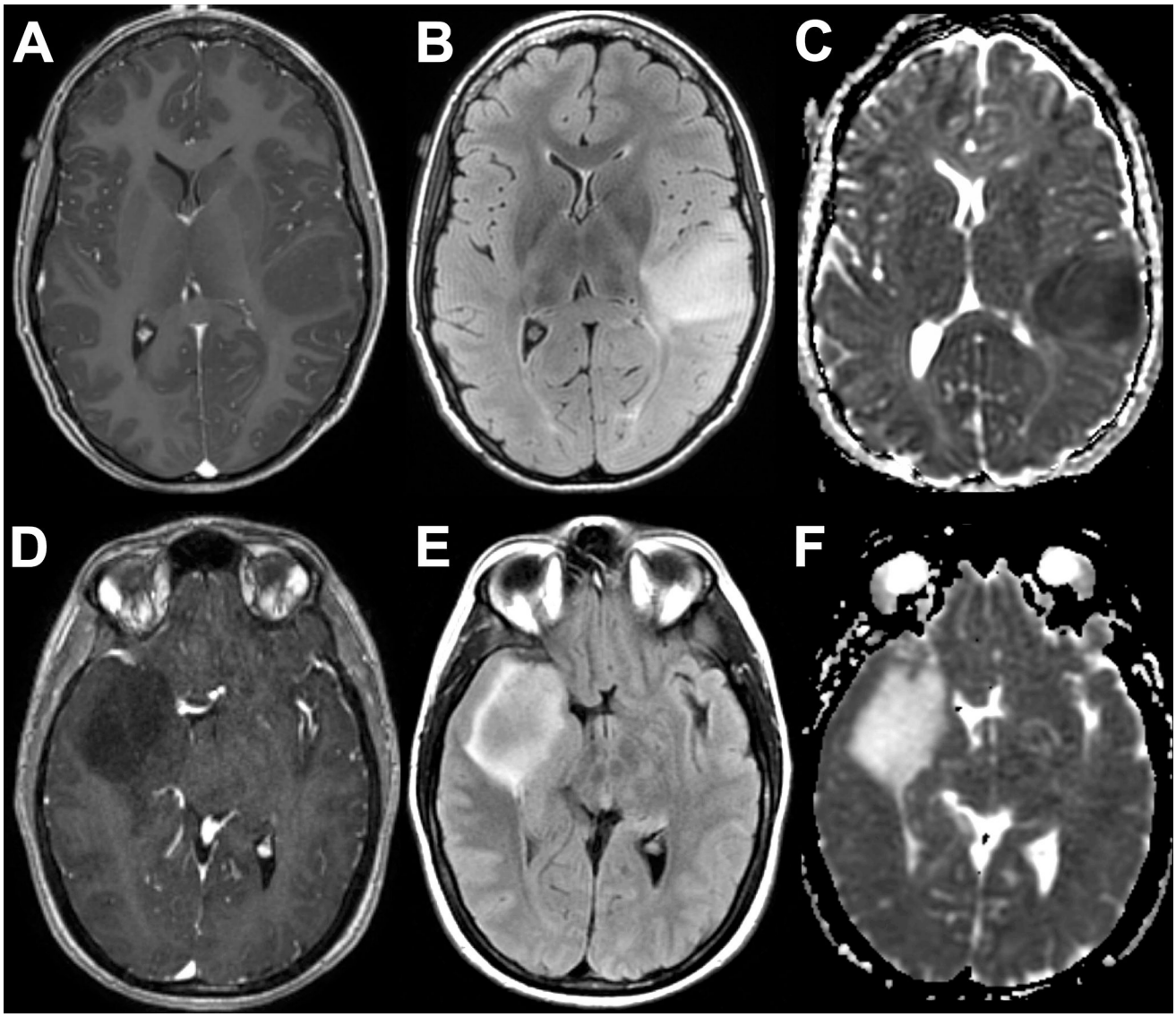

Fig. 1.

Representative MRIs of *IDH*-wildtype (A–C) and *IDH*-mutant (D–F) grade II DGs. 23-year-old woman with left frontoparietal opercular non-enhancing (A) and FLAIR hyperintense (B) mass with reduced diffusion on ADC (C). 45-year-old man with righ temporal non-enhancing (D) and FLAIR hyperintense (E) mass with facilitated diffusion on ADC (F).

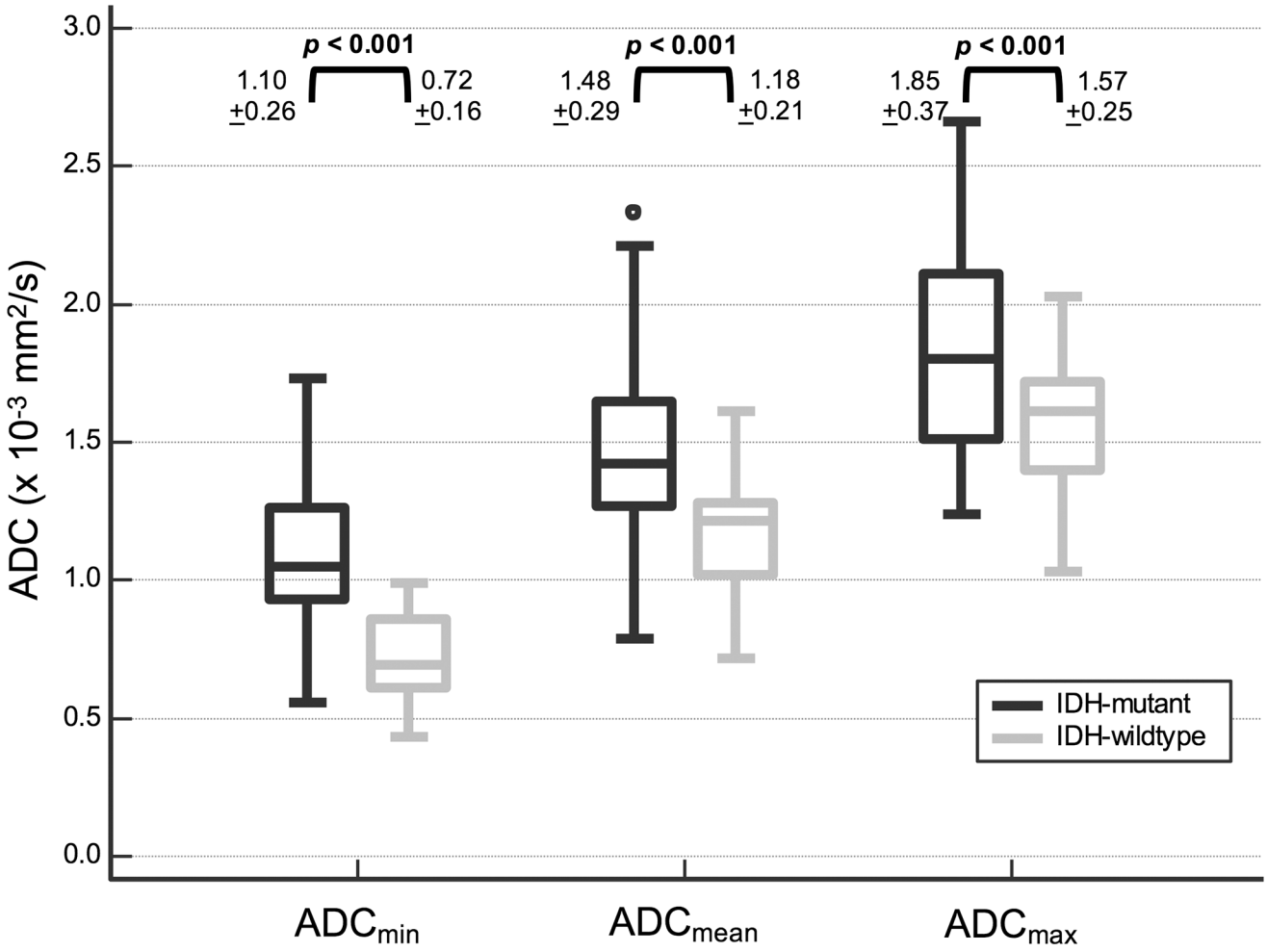

Fig. 2.

Boxplots of diffusion values in patients with *IDH*-mutant and *IDH*-wildtype grade II DGs demonstrate lower ADC values in *IDH*-wildtype tumors.

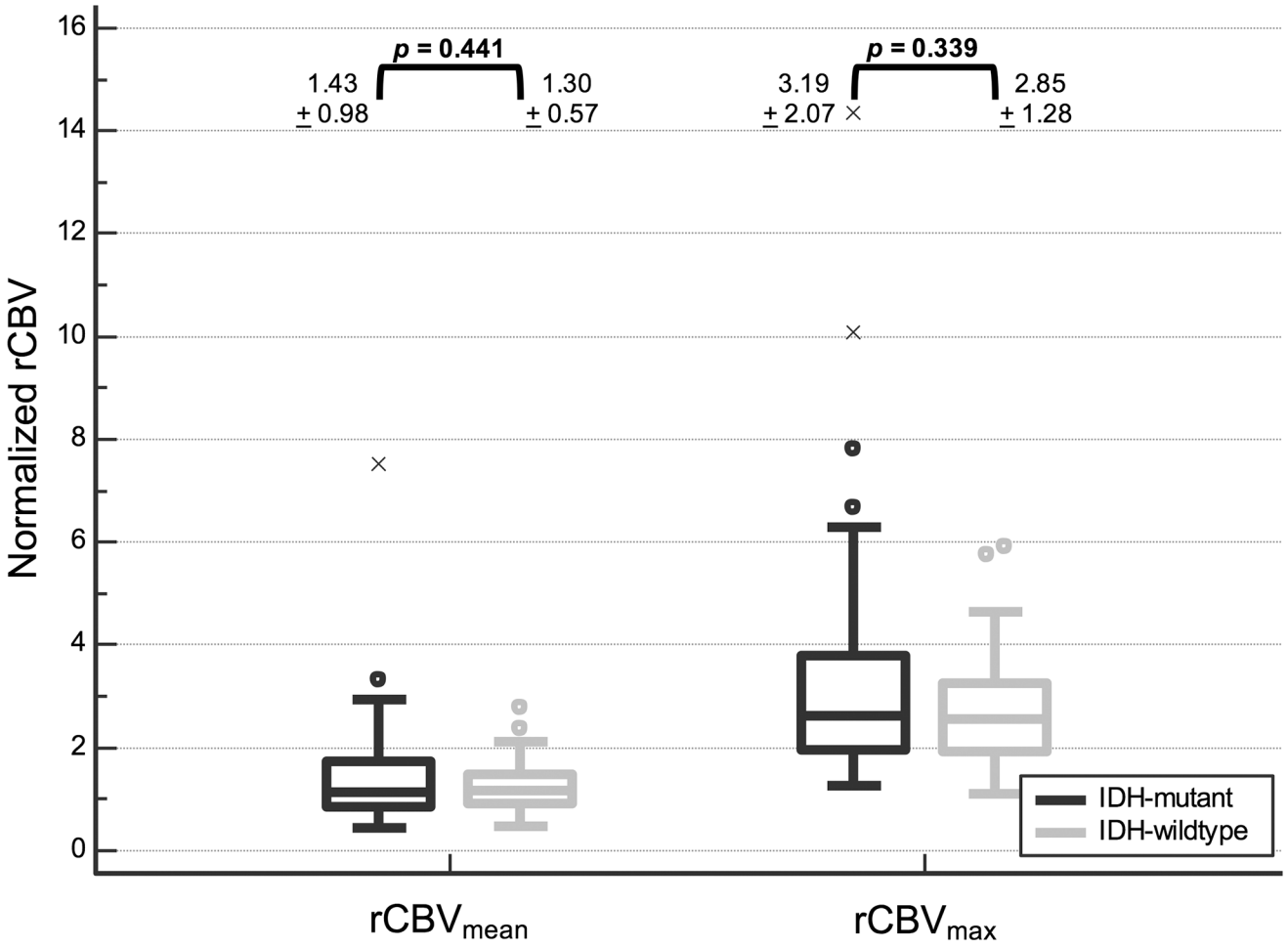

Fig. 3.

Boxplots of perfusion values in patients with *IDH*-mutant and *IDH*-wildtype grade II DGs demonstrate no significant difference in perfusion metrics between the two groups.

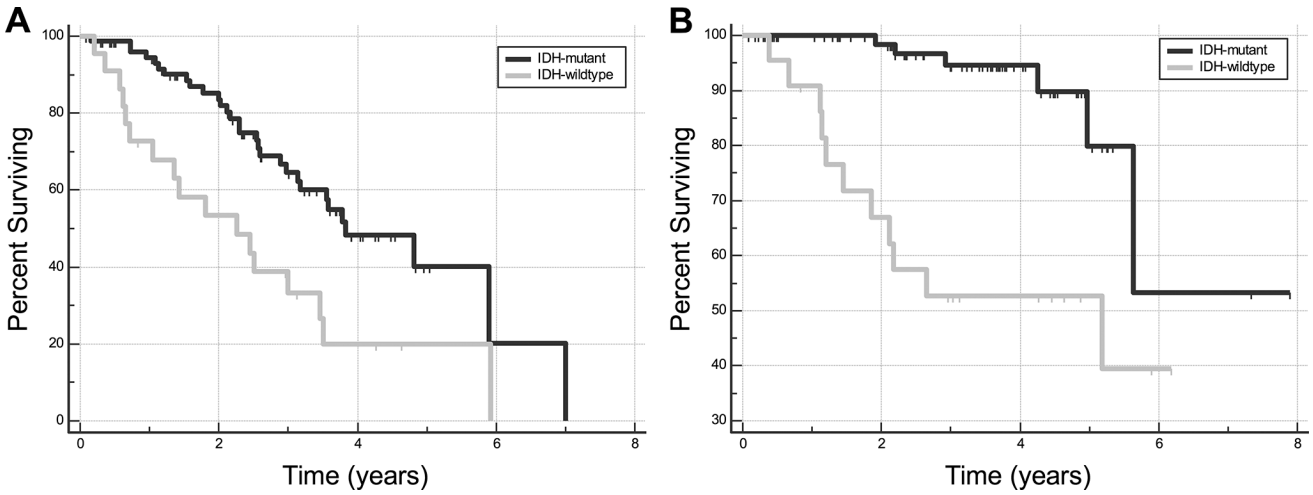

Fig. 4.

Kaplan-Meier curves for progression free survival (A) and overall survival (B) for patients with *IDH*-mutant and *IDH*-wildtype grade II DGs show longer survival for *IDH*-mutant tumors.

Table 1

MRI characteristics

Characteristic [n (%)]	*IDH*-mutant (n = 78)	*IDH*-wildtype (n = 22)	*p*-value
Multicentric	3 (4)	1 (5)	0.883
Multifocal	11 (14)	10 (45)	0.004
Location[1]			
Lobar	66 (85)	16 (73)	0.333
Central	15 (19)	6 (27)	0.602
Brainstem	0 (0)	6 (27)	< 0.001
Cortical involvement	63 (81)	13 (59)	0.069
Infiltrative edema	40 (51)	16 (73)	0.122
Mineralization or hemorrhage	21 (27)	4 (18)	0.577
Cystic change	23 (29)	1 (5)	0.033
Contrast enhancement	20 (26)	6 (27)	0.878

[1]Location total may be greater than cohort total due to tumor involvement of multiple locations